Proc. Natl. Acad. Sci. USA
Vol. 85, pp. 7557–7561, October 1988
Biophysics

Accurate simulation of protein dynamics in solution

(deviation from x-ray crystal structure/fluctuation amplitudes/hydrogen-bond stability)

MICHAEL LEVITT* AND RUTH SHARON

Department of Chemical Physics, Weizmann Institute of Science, Rehovot 76100, Israel

Communicated by A. Klug, June 23, 1988

ABSTRACT **Simulation of the molecular dynamics of a small protein, bovine pancreatic trypsin inhibitor, was found to be more realistic when water molecules were included than when *in vacuo*: the time-averaged structure was much more like that observed in high-resolution x-ray studies, the amplitudes of atomic vibration in solution were smaller, and fewer incorrect hydrogen bonds were formed. Our approach, which provides a sound basis for reliable simulation of diverse properties of biological macromolecules in solution, uses atom-centered forces and classical mechanics.**

Computer simulation is an essential tool for the study of all molecular systems too complicated to tackle by more analytical methods. The first simulation of the molecular dynamics of a small protein *in vacuo* led to a dramatic change in our view of protein dynamics, showing as it did a rich variety of large-amplitude motion on the picosecond time scale (1). When presented in a motion picture made by computer graphics, these calculated trajectories showed the nature of the motion vividly (2).

Although *in vacuo* simulations furthered the understanding of protein motion on the atomic scale, these calculations (1, 3–6) have a number of serious shortcomings: (*i*) the deviation of the time-averaged structure from the known x-ray structure of the protein is unacceptably large (>2 Å all-atom rms; 1 Å = 0.1 nm); (*ii*) the amplitude of internal motion calculated over a few picoseconds is no smaller than the amplitude of combined internal and external motion observed in crystals over much longer times; and (*iii*) many additional hydrogen bonds are formed.

Previous simulations of protein dynamics in hydrated crystals or in solution have attempted to correct the deficiencies of *in vacuo* simulations, doing pioneering work in the simulation and analysis of these much larger systems. The first simulation of crystals of bovine pancreatic trypsin inhibitor (BPTI) (7), done at the same time as the first *in vacuo* simulations of BPTI (8), lasted only 2 ps. Continued simulation of this system with better equilibration (9) and for longer times (10) still gave a relatively large rms deviation of all atoms from the x-ray structure (>1.8 Å at 40 ps), in spite of the stabilizing effect of the crystal lattice. There have been several simulations of proteins in solution. The first study (4) simulated BPTI protein for 25 ps in a box of 1460 carbon atoms, which is a poor model for water. The second study simulated BPTI in a truncated octahedron of 1462 water molecules for only 20 ps (11), after which time the rms deviation was high (2.7 Å). The third study simulated the active site of ribonuclease in a droplet of water (12) and did not aim to reproduce the properties of protein in solution. The fourth study simulated trypsin for 42 ps in a box of 4785 water molecules but has only been analyzed in a preliminary way and gives too high a diffusion constant for the bulk water (13). The earliest account of the present work (14) gave too large a rms deviation, 2.3 Å, after 40 ps.

Convinced that inclusion of water molecules should improve simulations, we persevered with the simulation of the BPTI in solution. This protein was chosen because of its small size (58 residues), the high-resolution x-ray (15, 16) and neutron (16) crystal structures, and its use in other simulations (1–11, 14). In completing this study we have had to (*i*) modify a three-point water model to allow for internal flexibility and better reproduce the structure of real water, (*ii*) eliminate discontinuities from the force calculation so that the total energy of the entire system remains constant without requiring velocity adjustment, (*iii*) include all hydrogen atoms and the net charges on ionizable groups, (*iv*) include enough water molecules to approximate solution, (*v*) run the trajectory for sufficiently long, and (*vi*) analyze the simulation in sufficient detail so as to be able both to detect and correct errors and to comprehend the equilibrium and kinetic properties of such a complicated system. Our calculation, which uses a simple atom-centered potential and classical mechanics to simulate a trajectory lasting 210 ps, shows that inclusion of solvent improves the agreement with experiment and gives insight into protein–water interactions.

We find that in solution, the time-averaged protein structure is much more like that observed in high-resolution x-ray studies of BPTI (rms deviation is 1.1 Å as opposed to 1.9 Å *in vacuo*) and there are fewer incorrect hydrogen bonds (1 as opposed to 14 *in vacuo*). A shell of water molecules with higher than normal density (1.25 g/ml) and reduced rotational freedom is found close to the protein surface.

Form of the Potential

The potential-energy function used in this work was chosen to fulfill the somewhat contradictory goals of maximum realism and greatest simplicity. Realism, because we are attempting to reproduce accurately the dynamic properties of a globular protein in solution. Simplicity, because even a small protein surrounded by its complement of water molecules constitutes a very large molecular system with almost 10,000 atoms. We chose to (*i*) include all hydrogen atoms, as a water molecule without its hydrogen atoms is quite unrealistic; (*ii*) avoid using any interaction centers not centered on atomic nuclei (for example, lone-pair electron orbitals), as this would require significantly more computer time; (*iii*) allow all degrees of freedom, even those internal to a water molecule, as this improves the accuracy of pure water simulations (unpublished results), treats bond angles equivalently in the protein and in the solution, and does not require significantly more computer time (5).

The interatomic potentials used here are those developed by the Lifson group over the past 20 years (17–19). Bonded terms include bond lengths and bond angles treated as harmonic springs and torsion angles treated as periodic functions. Nonbonded terms, which are calculated between

The publication costs of this article were defrayed in part by page charge payment. This article must therefore be hereby marked "*advertisement*" in accordance with 18 U.S.C. §1734 solely to indicate this fact.

Abbreviation: BPTI, bovine pancreatic trypsin inhibitor.

*Present address: Department of Cell Biology, Stanford University, Stanford, CA 94305.

pairs of atoms further apart than three bonds, include Lennard–Jones potentials ($A/r^{12} + B/r^6$) for van der Waals interactions and Coulomb potentials (q_iq_j/r) for electrostatic interactions. The force constants have been published (5) except for those of the water molecule, for which we use a flexible three-point water model (a full description of this water model and of the potential will be published elsewhere). This model, known as F3P, is based on the SPC (20) and TIPS (21) models and works as well as more complicated water models (22) in reproducing a wide range of thermodynamic, kinetic, and structural properties of pure water. Independent simulations using a flexible SPC water model confirmed these findings (23).

Preliminary experiments indicated that for a system consisting of two components, like the protein and water molecules we have here, special care must be taken to integrate the equations of motion accurately. In particular, it is important to ensure that the total energy of the microcanonical ensemble is conserved: correcting the energy by rescaling the velocities, which has been successfully applied to single-component systems (3, 5), can lead to serious temperature imbalance in multicomponent systems. We eliminated this imbalance by smooth and continuous truncation of nonbonded interactions between neutral groups of atoms at a range of 7 Å. Such neutral-group smoothing, which has been described (24), has not been widely used for simulations of protein dynamics.

The net charges of ionizable carboxyl and amino groups were set to $-1e$ and $+1e$, respectively. Due to an oversight, the guanidinium group of each arginine side chain was not given a net charge of $+1e$; under these circumstances, the protein is electrically neutral and no counterions need to be introduced.

Periodic boundaries, which ensure that every water molecule sees a full complement of surrounding water molecules and that a water molecule leaving one side of the box immediately reenters on the opposite side, were set up by surrounding the protein and water with a rectangular box. The box, which was chosen to be 8 Å bigger than the protein in all directions, has dimensions of 48.5 Å × 42.4 Å × 42.2 Å = 86,764 Å^3 and contains 2607 water molecules (7821 atoms) and 892 protein atoms (a total of 8713 atoms and 26,139 degrees of freedom). At 37°C, each water molecule has a volume of 30.09 Å^3, so that the volume occupied by the protein is 8319 Å^3 [86,764 − (2607 × 30.09)] and the specific volume is 0.77 ml/g, in agreement with the expected value of 0.73 ml/g (25).

As in previous work (5), we first equilibrate by energy minimization of the x-ray structure surrounded by the modeled solvent and then use the Beeman method (26) to integrate the equations of motion with a 2-fs time step at 310 K for 210 ps in vacuum and in solution. Because energy discontinuities and spurious forces are removed by smooth truncation, energy is well-conserved even in solution and velocities need not be rescaled (by 0.975) more often than once every 30,000 steps (60 ps).

Overall Properties

The simplest way to judge whether the simulation is realistic is to determine the extent to which the motion causes a breakdown of the x-ray structure. In vacuum, it takes about 60 ps before the rms deviation from the starting structure reaches a stable value, whereas in solution, the structure settles down more quickly (30 ps) and remains closer to the x-ray structure (29) (Fig. 1). After 210 ps the deviation is 2.4 Å *in vacuo* and 1.4 Å in solution. The rms deviations of the structures obtained by averaging the coordinates over the last 100 ps of the trajectory are smaller, 2.07 Å *in vacuo* and 1.18 Å in solution. The deviation of the mean structure *in vacuo* is smaller than for previous *in vacuo* results, and the value in solution is smaller than previous results in solvent or in the crystal lattice (Fig. 1).

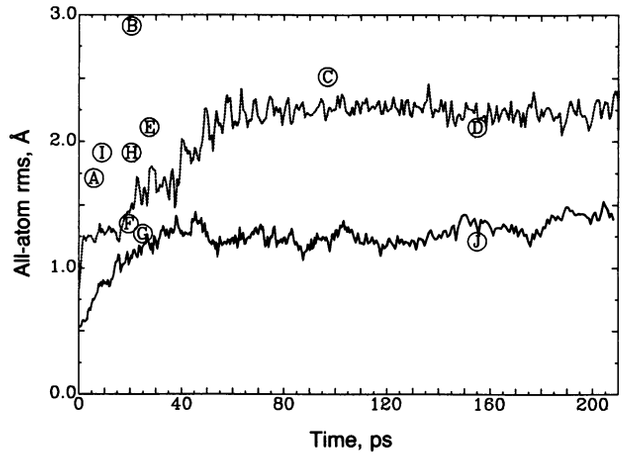

FIG. 1. Time dependence of the rms deviation of all 454 non-hydrogen atoms from the x-ray structure of BPTI (4PTI) for simulations *in vacuo* (dotted line) and in solution (solid line). The rms deviations of the time-averaged structures obtained in this and other BPTI simulations are marked as circled capital letters plotted at the midpoint of the averaging period: A, first *in vacuo* simulation averaged over a period of 3–9 ps (1); B, *in vacuo* for 15–40 ps (4); C, *in vacuo* for 62–132 ps (5); D, *in vacuo* for 110–210 ps (present work); E, in fixed crystal lattice for 15–40 ps (4); F, form I crystal for 19–20 ps (9); G, form II crystal for 10–40 ps (10); H, in nonpolar solvent for 8–33 ps (4); I, in water octahedron for 2–20 ps (11); J, in water for 110–210 ps (present work).

In solution, the positional deviation of the main chain from the crystallographic structure is larger than that between the two crystal forms (29) (0.77 Å as opposed to 0.44 Å; Table 1); this could be due to defects in the energy parameters or to differences between the crystal and solution structures. Simulations of BPTI in the crystal should resolve this question; previous simulations of crystals (9, 10) gave larger rms deviations than found here in solution.

In vacuo the side chains show particularly large rms deviations (2.5 Å as opposed to 1.4 Å in solution). The radius of gyration is about 5% smaller *in vacuo* than in solution or observed experimentally in the crystal.

Amplitudes of Motion

Amplitudes of backbone and side-chain fluctuation are smaller by 30% in solution than *in vacuo* (Table 1). This may seem a cause for concern, as the agreement with the experimental amplitudes of motion deduced from the crystallographic temperature factors (B values) has generally been used to support the accuracy of *in vacuo* protein dynamics simulations (1–6). The B value, which indicates the spread of the atomic electron density during the time the crystal is exposed to the x-ray beam (many minutes), will be increased both by motion and disorder of the protein molecule as a rigid body in the crystal lattice and by motion and disorder internal to the protein molecule.

The amplitudes calculated in simulations of protein dynamics *in vacuo* or in solution relate only to internal motion of the protein itself; no account is taken of rigid-body motion or disorder. Significant contributions of rigid-body lattice motions have been observed in cytochrome *c'* crystals (27). Lattice motions in protein crystals have recently been observed directly (28).

We feel that the smaller amplitudes calculated here are a better indication of the true extent of internal motion: proteins in solution are, therefore, more rigid and remain

Table 1. Comparison of overall accuracy of *in vacuo* and solution simulations

Property	*In vacuo**	In solution	Experimental
rms deviation (Å)†			
All-atom	1.91	1.13	1.10
C^α	1.01	0.74	0.44
Main-chain	1.06	0.77	0.44
Side-chain	2.50	1.40	1.50
Radius of gyration (Å)‡	10.93	11.51	11.53
Fluctuation (Å)§			
C^α	0.55	0.42	0.65
C^β	0.64	0.50	0.68
C^γ	0.81	0.54	0.85
C^δ	1.09	0.67	1.02
Hydrogen bonds			
Number formed	27¶	20¶	21‖
Number correct	17	20	21
Mean stability**	64	68	—

*Time-averaged values were calculated over the period 105–210 ps.
†The rms deviation of the time-averaged structure was calculated relative to the form I BPTI x-ray coordinates [Brookhaven data set 4PTI with R factor = 17% at 1.2-Å resolution (15)] for only residues 1–56, as the chain termini are poorly resolved in the crystal. The all-atom value was calculated after best superposition of 444 non-hydrogen atoms; the C^α, main-chain, and side-chain values were then calculated. The experimental deviations were calculated in the same manner between the coordinate sets of forms I and II [4PTI (15) and 5PTI (16), respectively].
‡The radius of gyration of the protein, R_g, was computed as $R_g = [n^{-1}\Sigma(|r_i - r_{cm}|)^2]^{1/2}$ for all the non-hydrogen atoms.
§The simulated fluctuation value was averaged over the relevant atoms of residues 2–56 (rms). The experimental fluctuation value was calculated from the mean temperature factor, B, of the same atoms in the 4PTI data set by using the relationship $(3B/8\pi^2)^{1/2}$.
¶Only those peptide–peptide hydrogen bonds that are formed (O···H distance < 2.6 Å and O···N—H angle < 35°) for >10% of the analysis period were considered.
‖Two x-ray-structure hydrogen bonds (29) with O···N—H angles >45° are not included (27,H···24,O and 44,H···42,O).
**The hydrogen-bond stability calculated from the simulation is the percentage of the 100-ps analysis period for which the bond is formed.

closer to a mean structure than suggested by previous simulations or extrapolations from crystallographic B values.

Hydrogen Bonds

The main-chain hydrogen bonds in the solution simulation are much more like those found experimentally in native BPTI crystals. In solution, only 1 native hydrogen bond is not found [the interaction, 16,H···36,O, is also absent *in vacuo* and in other simulations (5, 10, 11)]. *In vacuo*, 4 native hydrogen bonds are not found and there are 10 extra hydrogen bonds, giving a total of 14 errors. Although different hydrogen bonds have different stabilities, the individual stabilities *in vacuo* and in solution are remarkably similar (mean values of 64% and 68%, respectively, and correlation coefficient of 0.74). Because every water molecule can make strong hydrogen bonds to both the >NH and >CO groups of the peptide, one may have expected the water molecules to have a much greater effect on hydrogen-bond stability. In 100 ps, the protein structure does not open up enough to enable a water molecule to come between hydrogen-bonding groups, so that the strength of hydrogen bonds is the same as *in vacuo*.

Effect of Protein on Water

The most dramatic effect of the protein is to more than double the number of water molecules in contact with polar and nonpolar surface relative to that expected from the accessible surface area (30) (Fig. 2*a*). This clustering of water molecules close to the protein surface increases to 1.25 g/cm³ the water density within 3–4.25 Å of the protein surface (Fig. 2*b*), mainly due to the large number of water molecules that are 3.75 Å from nonpolar atoms. Such increased density, which is a major effect involving about 150 water molecules (0.42 g of water per g of protein), has been observed at a flat nonpolar surface (32) and should also be visible in well-refined electron-density difference maps of protein crystals containing sufficient water. The density calculated from the Voronoi polyhedra volume per water molecule (Fig. 2*b*, dashed line) shows a small increase in density for the water molecules 2.5 Å from polar groups due to electrostriction and a small decrease in density for the water molecules 3–4.5 Å from the surface. The near constancy (within 5%) of the Voronoi-derived density indicates that although water molecules are clustered perpendicular to the protein surface, they are not brought closer together parallel to the surface.

For a more detailed analysis of the way the protein changes the properties of the surrounding water molecules, it is convenient to divide the water molecules into four classes according to their distance from the protein surface (Table 2; Fig. 3). More than half the water molecules are in class IV. These water molecules, which are further than 10 Å from the nearest protein atom, have properties that are indistinguishable from those calculated for pure water (ref. 23 and unpublished data). Their diffusion coefficient of 0.24 Å²/ps agrees with the experimental diffusion coefficient of water

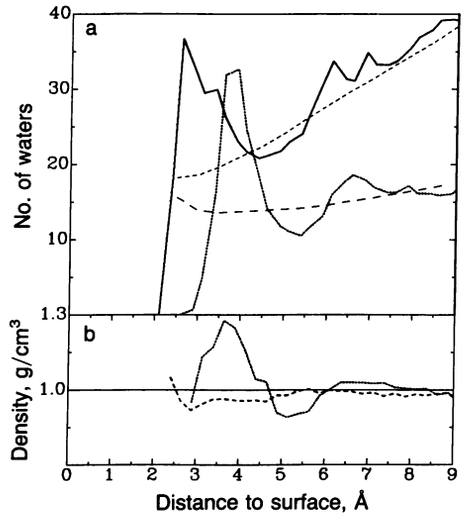

FIG. 2. The number of water molecules and the water density vary with distance from the protein surface (distance from a water oxygen to the closest non-hydrogen atom of the protein). (*a*) The number of water molecules counted during the simulation is shown separately for those closest to a polar atom (——) and those closest to a nonpolar atom (·····). The expected number of water molecules, shown separately for polar (----) and nonpolar (– – –) surface, was calculated from the surface area of shells 2–9 Å from the protein. (*b*) The density was calculated in two ways. The first method used Richard's Voronoi polyhedra program (31) to calculate the instantaneous volume of each water molecule (----). Averaging this volume for all water molecules within a given distance gives the mean density per molecule for each shell. The second method recorded how often during the simulation the oxygen of each water molecule was in a particular 1-Å³ volume element around the protein (after protein rigid-body motion was removed); the distance from the protein surface of each of the volume elements only occupied by water was calculated by using the time-averaged protein structure (·····). Both the density and the number of water molecules were averaged over the period 110–210 ps.

Table 2. Properties of water molecules in classes I–IV

Property	I	II	III	IV
Number of waters	107	124	1007	1368
D (Å^2/ps)*				
End	0.10	0.15	0.19	0.24
Start and end	0.06	0.10	0.18	0.24
Energy†				
Bond stretching	2.00	1.62	1.62	1.61
Angle bending	0.62	0.58	0.57	0.58
Water–water	−12.68	−22.35	−23.98	−24.28
Water–protein	−14.02	−2.33	−0.57	−0.12
Binding‡	−24.08	−22.48	−22.35	−22.21
Binding (relative to bulk water)	−1.87	−0.27	−0.15	0.0
Total§	−10.73	−10.14	−10.08	−10.01

*The diffusion constant of a water molecule was calculated from Δr, the change in position of the oxygen atom occurring in time t, by using $\langle \Delta r^2 \rangle / 6t$. Because a water molecule initially in a given class may leave during this time, calculation of class-averages is not straightforward. Two methods were used: (*i*) consider only those water molecules that are in the particular class at the end of the analysis period; (*ii*) consider only those water molecules that are in the particular class at the start and end of the analysis period.

†Energy is measured in kcal/mol of water molecule (1 kcal = 4184 J).

‡Binding energy (bond + angle + water–water + water–protein) is the energy lost when one water molecule is removed from the system without allowing anything else to rearrange.

§Total energy [bond + angle + 0.5(water–water + water–protein)] is the contribution made by one water molecule to the total energy of the system.

(0.26 Å^2/ps at 300 K) and is much smaller than the value of 0.45 Å^2/ps found in a simulation of trypsin in solution (13).

The 107 water molecules in class I, which are in contact with polar groups, are most affected by the protein. These water molecules interact strongly with the protein and, as a consequence, have slightly more strained bonds and angles (by 0.39 and 0.04 kcal/mol, respectively) and much less favorable interactions with other water molecules (by 11.6 kcal/mol). Because they interact so favorably with the protein (−14.02 kcal/mol), class I water molecules have lower binding energies than bulk water (−1.9 kcal/mol). The strong interaction of class I (magenta) water molecules with >CO, $-COO^-$, and $-NH_3^+$ groups is clearly seen in Fig. 3.

The 124 water molecules in class II, which are all in contact with nonpolar groups, have their diffusive motion restricted almost as much as those in class I. Class II water molecules do not interact very strongly with the protein (−2.33 kcal/mol) and their binding energies are only slightly lower than in bulk water (−0.27 kcal/mol).

The lowered binding energy of water molecules in classes I and II is offset by a decrease in the entropy associated with their restricted translation and rotation. This can be quantified by comparing the distributions of water position and orientation with that expected for a completely unstructured solvent. The entropic contribution to the Gibbs energy is $-kT \Sigma n_i \ln \rho_i$, where kT is Boltzmann's constant times absolute temperature, n_i is the observed number, and ρ_i is the ratio of n_i to the number expected for a uniform distribution. For the translational entropy, we compare the actual number of water molecules found in radial shells with that expected from the accessible surface (Fig. 2*a*); this gives a total Gibbs energy change of 10 kcal/mol for the polar surface and 31 kcal/mol for the nonpolar surface. The distribution of the angle between a water O—H bond and the normal to the protein surface shows that for the polar surface, angles of 0° and 105° are strongly preferred, which gives a total Gibbs energy change of 74 kcal/mol, whereas for the nonpolar surface, the preferred angle is 70°, which gives a change of 17 kcal/mol. Adding the two contributions gives a Gibbs energy change per water molecule of 0.8 kcal/mol for class I and 0.4 kcal/mol for class II. The binding Gibbs energy, which includes the entropic terms, indicates that whereas water molecules bind favorably to polar atoms (by −1.08 kcal/

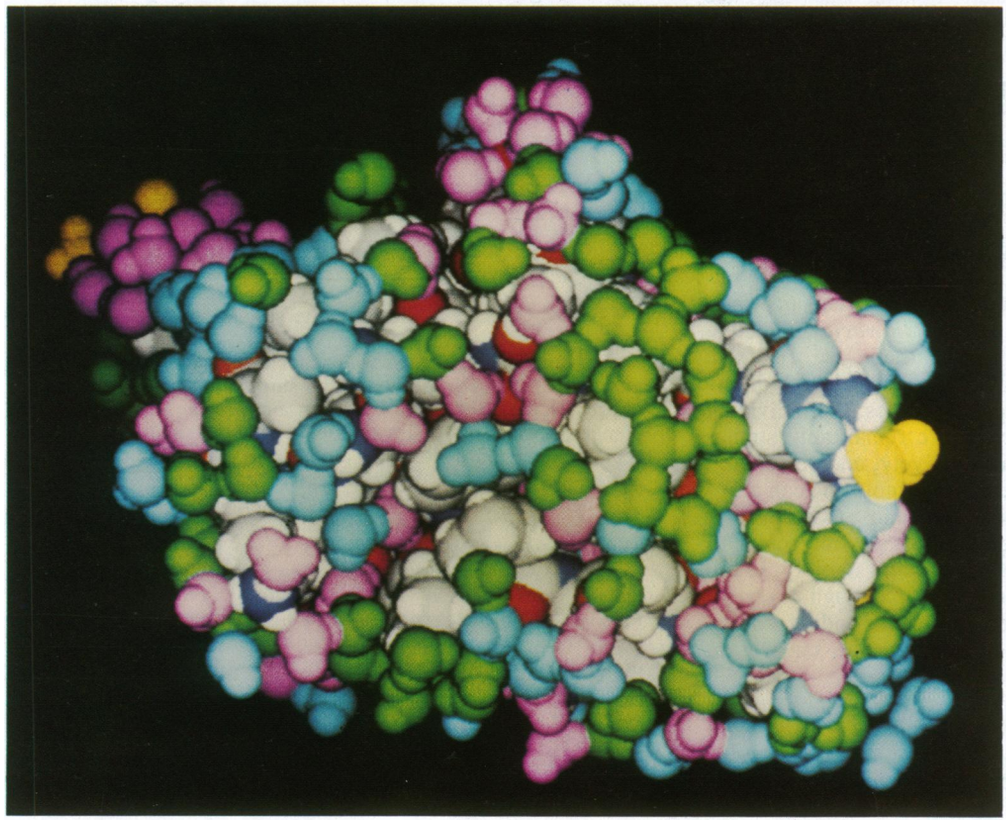

FIG. 3. Water molecules within 4 Å of the protein surface at an arbitrarily selected time (61.5 ps). The 2607 water molecules are divided into four mutually exclusive classes and colored as follows. Class I: magenta, <3.2 Å from a polar atom of the protein (O or N). Class II: green, <4.5 Å from a nonpolar atom of the protein (C or S). Class III: cyan, not in classes I, II, or IV. Class IV: yellow, inside the volume bounded by the box sides and an ellipsoid that just fits into the box. Normal Corey–Pauling–Koltun colors are used for the other atoms (red, O; blue, N; yellow, S; gray, C; white, H).

mol), their interaction with nonpolar atoms is slightly unfavorable (by 0.12 kcal/mol).

Water molecules are very mobile and move from class to class during the simulation. Because class I and II water molecules are in adjacent patches on the protein surface, the average time that a water molecule spends in each class is short, 4 ps for class I and 1 ps for class II (10 tightly bound water molecules remain in class I for the entire 100-ps period analyzed). Water molecules keep on leaving and then returning to a given class so that after 100 ps, 34% of the molecules originally in class I are still in it, whereas the corresponding number for class II is 12%. Although any structure (Fig. 3) associated with class II water molecules will be short-lived, it will have a high probability of being reformed again by the same water molecules.

Why Is Simulation Better in Solution?

This work shows that molecular dynamics simulation of protein motion is more realistic when solvent is included, in that the structure remains closer to the x-ray structure and the amplitudes of vibration are smaller. This improvement can arise from thermodynamic and kinetic factors, in that the solvent can alter both the effective potential between protein atoms and the rates of energy exchange.

The effective potential is altered by solvent in two ways: (*i*) the removal of the protein/vacuum interface eliminates the surface pressure, which causes the shrinkage of the radius of gyration *in vacuo* (Table 1); (*ii*) the possibility of hydrogen bonding to water molecules eliminates the spurious additional hydrogen bonds that occur *in vacuo*. The small amplitudes of atomic motion and the high stability of hydrogen bonds found in the present work indicate that in solution the protein Gibbs energy increases as rapidly with deviation from native structure as *in vacuo*. This means that for small perturbations a protein in solution has a similar effective potential as *in vacuo*. It is only when the protein groups are moved sufficiently far apart to admit water that the perturbed structure in solution becomes less stable due to favorable interactions with these water molecules.

Rates of energy exchange will be altered by the viscous damping of the solvent. In particular, equilibration could be much slower *in vacuo* due to the slower exchange of energy. After the initial warming-up period, there may be a small energy imbalance in which several of the low-frequency modes have more than their fair share of thermal energy. As a result, these modes will move more, causing the entire structure to move from the starting structure (33). In solution, a similar initial imbalance will quickly be corrected because solvent damping promotes rapid energy exchange. This phenomenon is akin to gently placing a bell on a hard surface. In vacuum, the initial shock, however slight, will cause the bell to ring for a time. Repeating the experiment in water will cause much less ringing, due to damping.

Provided that care is taken to eliminate energy discontinuities, include all hydrogen atoms, include sufficient solvent, and run for more than 60 ps, a reasonable level of realism can be obtained by using published energy functions. Quantum effects, which have been found to have a small effect on most of the properties of liquid water (34), are expected to be of little importance in determining equilibrium or kinetic properties of proteins in solution. As calculations become more accurate, involving larger systems and longer times, these effects may become important. For the present, molecular dynamics simulations in solution with simple atom-centered potentials and classical dynamics reproduce with good quantitative accuracy a wide range of experimental observations. These methods will be useful for further detailed study of macromolecular dynamics in solution.

We thank Drs. B. Brooks, A. Klug, I. D. Kuntz, S. Lifson, and F. M. Richards for critical discussion. This work was supported by the U.S.–Israel Binational Science Foundation. Access to the Cray X-MP at the San Diego Supercomputer Center was generously provided by National Science Foundation Award DMB 85-10935 and San Diego Supercomputer Center Award DMB 87-0015S. Much of the analysis was done while M.L. was a guest at the Medical Research Council Laboratory of Molecular Biology (Cambridge, England).

1. McCammon, J. A., Gelin, B. R. & Karplus, M. (1977) *Nature (London)* **267**, 585–590.
2. Levitt, M. & Feldmann, R. J. (1981) in *Structural Aspects of Recognition and Assembly in Biological Macromolecules*, ed. Balaban, M. (Elsevier/North-Holland, The Netherlands), pp. 35–56.
3. Karplus, M. & McCammon, J. A. (1981) *CRC Crit. Rev. Biochem.* **9**, 293–349.
4. van Gunsteren, W. F. & Karplus, M. (1982) *Biochemistry* **21**, 2259–2274.
5. Levitt, M. (1983) *J. Mol. Biol.* **168**, 595–620.
6. Levitt, M. (1983) *J. Mol. Biol.* **168**, 621–657.
7. Hermans, J. & Rahman, A. (1976) in *Models for Protein Dynamics*, ed. Berendsen, H. J. C. (CECAM, Universite de Paris IX, France), pp. 153–158.
8. McCammon, J. A. (1976) in *Models for Protein Dynamics*, ed. Berendsen, H. J. C. (CECAM, Universite de Paris IX, France), pp. 137–152.
9. van Gunsteren, W. F., Berendsen, H. J. C., Hermans, J., Hol, W. G. J. & Postma, J. P. M. (1983) *Proc. Natl. Acad. Sci. USA* **80**, 4315–4319.
10. Berendsen, H. J. C., van Gunsteren, W. F., Zwinderman, H. R. J. & Geurtsen, R. G. (1986) *Ann. N.Y. Acad. Sci.* **482**, 268–286.
11. van Gunsteren, W. F. & Berendsen, H. J. C. (1984) *J. Mol. Biol.* **176**, 559–564.
12. Brunger, A. T., Brooks, C. L. & Karplus, M. (1985) *Proc. Natl. Acad. Sci. USA* **82**, 8458–8462.
13. Wong, C. F. & McCammon, J. A. (1987) *Isr. J. Chem.* **27**, 211–215.
14. Levitt, M. & Sharon, R. (1987) in *Crystallography in Molecular Biology*, eds. Moras, D., Drenth, J., Strandberg, B., Such, D. & Wilson, K., NATO ASI Series A (Life Sciences, Pergamon, New York & London), Vol. 126, pp. 197–207.
15. Deisenhofer, J. & Steigemann, W. (1975) *Acta Crystallogr.* **B31**, 238–250.
16. Wlodawer, A., Walter, J., Huber, R. & Sjölin, L. (1984) *J. Mol. Biol.* **180**, 301–331.
17. Warshel, A. & Lifson, S. (1970) *J. Chem. Phys.* **53**, 582–594.
18. Levitt, M. & Lifson, S. (1969) *J. Mol. Biol.* **46**, 269–279.
19. Hagler, A. T., Huler, E. & Lifson, S. (1974) *J. Am. Chem. Soc.* **96**, 5319–5327.
20. Berendsen, H. J. C., Postma, J. P. M., van Gunsteren, W. F. & Hermans, J. (1981) in *Intermolecular Forces*, ed. Pullman, B. (Reidel, Dordrecht, The Netherlands), pp. 331–342.
21. Jorgensen, W. L. (1981) *J. Am. Chem. Soc.* **103**, 335–340.
22. Rahman, A. & Stillinger, F. H. (1971) *J. Chem. Phys.* **55**, 3336–3359.
23. Anderson, J., Ullo, J. J. & Yip, S. (1987) *J. Chem. Phys.* **87**, 1726–1732.
24. Brooks, B. R., Bruccoleri, R. E., Olafson, B. D., States, D. J., Swaminathan, S. & Karplus, M. (1983) *J. Comp. Chem.* **4**, 187–194.
25. Cohn, E. J. & Edsall, J. T. (1943) *The Proteins* (Academic, New York).
26. Beeman, D. (1976) *J. Comput. Phys.* **20**, 130–139.
27. Finzel, B. C. & Salemme, F. R. (1985) *Nature (London)* **315**, 686–688.
28. Doucet, J. & Benoit, J. P. (1987) *Nature (London)* **325**, 643–646.
29. Wlodawer, A., Deisenhofer, J. & Huber, R. (1987) *J. Mol. Biol.* **193**, 145–156.
30. Lee, B. & Richards, F. M. (1971) *J. Mol. Biol.* **55**, 379–400.
31. Richards, F. M. (1974) *J. Mol. Biol.* **82**, 1–14.
32. Lee, C. Y., McCammon, J. A. & Rossky, P. J. (1984) *J. Chem. Phys.* **80**, 4448–4455.
33. Levitt, M., Sander, C. & Stern, P. S. (1985) *J. Mol. Biol.* **181**, 423–447.
34. Kuharski, R. A. & Rossky, P. J. (1985) *J. Chem. Phys.* **82**, 5164–5177.